9

Research Article

Haider Ali Al-Tameemi, Haider A. A. Al-Katib* and Hayder H. Alkhudery

Experimental investigation on strengthening lap joints subjected to bending in glulam timber beams using CFRP sheets

https://doi.org/10.1515/eng-2022-0494 received June 08, 2023; accepted July 22, 2023

Abstract: Strengthening the carpentry joints is considered a big challenge for designers to maintain the joined timber elements' load transfer and integrity. This research work investigates different techniques to strengthen the lap joints in glulam timber beams using carbon fiber-reinforced polymer (CFRP) sheets. For this purpose, 12 specimens of glulam timber beams were tested using the four-point loading method. One of the glulam timber specimens was an intact nonlapped specimen, and the others were lapped at mid-span using half-height lap joints. The lap joints were strengthened using different configurations of the CFRP sheets. The test variables were the clamping scheme, bond length, and reinforcement ratio of the CFRP sheets. The analysis of the test results indicates that the CFRP strengthening configuration could be more effective in strengthening the lapped glulam timber beams when the reinforcement ratio of the longitudinal CFRP sheets was equal to 0.303%, and the wrapping CFRP sheets continued beyond the lapped joint by a distance equal to the beam height. Such a strengthening configuration could succeed in increasing the effective stiffness and ultimate load of the lapped timber specimen to 109 and 110%, respectively, relative to those of the intact nonlapped specimen. Moreover, the results reveal that increasing the length or the reinforcement ratio of the longitudinal CFRP sheets without increasing the width of the wrapping CFRP sheets could not succeed in achieving the required improvements in the structural behavior of the lapped timber beams.

Haider Ali Al-Tameemi: Department of Civil Engineering, University of Kufa, Najaf, Iraq, e-mail: hayder.altameemi@uokufa.edu.iq
Hayder H. Alkhudery: Department of Civil Engineering, University of Kufa, Najaf, Iraq, e-mail: hayder.alkhudhri@uokufa.edu.iq
ORCID: Haider Ali Al-Tameemi 0000-0002-7510-1354; Haider A. A. Al-Katib 0000-0003-4730-2797; Hayder H. Alkhudery 0000-0002-8401-4754

Keywords: CFRP sheet, glulam timber beams, lap joints, reinforcement ratio, wrapping sheet

1 Introduction

For ages, wood has been widely used as a structural member in the construction field due to its strength-toweight ratio, good availability, and ease of work compared to other construction materials [1-4]. Introducing the glued laminated (glulam) technique in producing timber elements increases their strength-to-weight ratio and makes it easy to produce timber elements with a wide variety of cross-sectional dimensions. However, in many cases, production and transportation issues limit obtaining the required length of glulam timber elements. To obtain the required large length of a timber element, it is necessary to splice two or more timber pieces together using carpentry joints [5,6]. In addition, the carpentry joints are commonly used to perform required interventions, repairing or strengthening works in the existing timber structures [1,4,7]. A carpentry joint is a connection technique that allows timber elements to be assembled together and provides a proper load transfer between them. There are many different forms of carpentry joints; the lap joint is considered one of the easiest forms to connect two timber pieces lengthwise. In the simple form of a lap joint, the interface plane is parallel to the axis of the joined pieces as the wood of one-half of the cross-section height or width of each piece is removed, as shown in Figure 1 [7,8]. The analysis of the whole timber structure is significantly influenced by the behavior of such joints [9]. One of the most critical issues in the design of timber joints is their ability in transfer internal forces between joined elements. The joints are mostly designed to carry axial and shear forces, but sometimes additional enhancements could be introduced to the joints to achieve a certain rotational restriction to carry bending moments [4,5]. However, the bearing capacity of timber structural members with unreinforced joints could never reach that of corresponding intact members [7,10].

^{*} Corresponding author: Haider A. A. Al-Katib, Department of Civil Engineering, University of Kufa, Najaf, Iraq, e-mail: hayder.alkatib@uokufa.edu.iq

2 — Haider Ali Al-Tameemi *et al.* DE GRUYTER

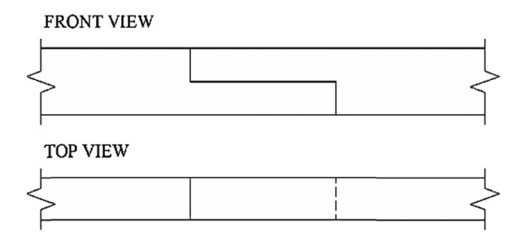


Figure 1: Simple lap joint [7,8].

The applicable standard (PN-EN 1995-1-1:2010) [9] does not specify any suggestions on how to conduct the right analysis with regard to the structural behavior of the carpentry joints. The current literature in this field is likewise incomplete. Perhaps since craftsmen in more recent times depended mostly on their personal experiences and own practice in this area, there are not enough thorough explanations of how the carpentry joints are made [7,8]. However, while describing the structural behavior of the carpentry joints provides the information needed to design appropriate solutions and interventions for timber connections, it is also necessary to describe the structural behavior of the entire structure. Therefore, research on carpentry joints' static behavior, repairs, and strengthening techniques is ongoing. In addition to this, it is pointed out that there is a lack in the number of studies that investigate the behavior of carpentry joints under the effect of bending moments [4,11]. Some of the studies done on the behavior of carpentry joints under bending are described briefly later.

Fajman and Máca [12–15] conducted a series of studies to investigate the effect of pins, keys, dovetails, the number of dowels, and the joint inclination on the structural behavior of scarf joints under bending. They suggested theoretical solutions to predict the effect of the number of dowels and the joint inclination on the structural behavior of scarf joints. Arciszewska-Kedzior et al. [16] utilized a scarf lap joint with inclined sides and dowels made of wood to restore the beam-end in ancient timber beams under bending. The authors concluded that the joint could be most efficient when it included three dowels and was located at the fifth of the beam's span from the support. Kunecký et al. [17,18] investigated experimentally and by means of the finite element method (FEM) the behavior of a lap timber joint with oblique sides and a dowel under bending. The authors stated that the joint's effective strength was between 55 and 60% of that of the reference solid beams. Karolak et al. [11] tested experimentally timber beams with carpentry joints of the type stop-splayed scarf joint under bending loads. They found that the timber beams strengthened with wooden pegs and additional steel clamps gave higher failure load and stiffness, while beams

strengthened with drawbolts gave the lower values. Ye et al. [10] strengthened the lap joints in standard timber beams of circular cross-section using carbon fiber-reinforced polymer (CFRP) bars, CFRP sheets, and steel bars in addition to drawbolts. The authors came to the conclusion that strengthening the joints using CFRP sheets gave better results than using CFRP bars or steel bras in terms of strength and stiffness. Karolak [8] investigated the behavior of different types of lap timber joints with different numbers of bolts under bending. According to the results of this study, timber beams with joints reached up to 40 and 60% of the reference intact beams' failure load and stiffness, respectively. It was also noticed that the main stress concentrations were found in the regions close to the bolt's holes. Karolak and Jasieńko [19] studied experimentally and using FEM the structural behavior of timber beams, including lightning sign scarf joints. They concluded that the vertically jointed beams had higher stiffness than the horizontally jointed beams. Patalas et al. [4] presented numerical analyses to study the structural behavior of stop-splayed scarf joints. On the basis of the results of this study, the authors expected that the extreme location of bolts, using additional clamping steel plates and strengthening the joint bottom surface using CFRP tapes, could significantly enhance the joint's loading resistance and stiffness.

FRP materials are synthetic composites produced using high-strength fibers [20,21]. The FRP reinforcing method was first introduced for strengthening concrete elements, as shown, for instance, by Kaiser [22], Ritchie et al. [23], and Saadatmanesh and Ehsani [24]. FRP composites are advantageous due to their high strength, elastic modulus, and resistance to corrosion. When it comes to reinforcing wood, CFRPs have various benefits. They have a low density, high durability, and easily adhere to wood. When the CFRP composites are connected to a tension face of a timber element, tensile stresses are transferred from the timber, allowing the compression fibers of the wood section to yield and better use the material's flexural capacity [25]. Beginning in 1992, CFRP was first used to reinforce timber [26,27]. Over the last three decades, many experimental, analytical, and computational studies have been conducted to learn more about the topic of timber reinforcement using CFRP materials. It was found that reinforcing timber members with CFRP materials improves their strength, ductility, and stiffness [25,28-30].

Yeboah and Gkantou [31] presented a general theoretical model to estimate the bending moment capacity of timber beams strengthened using FRP products based on assumption of the full bond between wood and FRP materials. According to this model, the theoretical resistance moment ($M_{\text{u.theoretical}}$) of timber beam section strengthened

with FRP materials can be calculated from the expression in equation (1) based on the equilibrium of the strengthened timber beam cross-section shown in Figure 2.

$$M_{\text{u,theoretical}} = F_{\text{wc1}} \left(d_{\text{c}} - \frac{1}{2} d_{\text{c1}} \right) + \frac{2}{3} F_{\text{wc2}} \cdot d_{\text{c2}} + F_{\text{fc}} \cdot a_{\text{fc}} + \frac{2}{3} F_{\text{wt}} \cdot d_{\text{t}} + F_{\text{ft}} \cdot a_{\text{ft}},$$
(1)

where F is an abbreviation for the subscript's force and dstands for the depth zone of the subscript. The subscripts w and f represent timber and FRP, respectively, and the subscripts c and t represent compression and tension, respectively. $a_{\rm fc}$ and $a_{\rm ft}$ stand for the arm of the FRP in compression and tension, respectively. While d_c is consisted of d_{c1} and d_{c2} for the plastic and elastic timber part region, respectively. Moreover, ε stands for the strain of the subscript and the subscripts y and u correspond to yield and ultimate state, respectively.

1.1 Research significance

The issue of strengthening the lap joints in the glulam timber beams considered a challenging for designers to maintain the joint load transfer and integrity to obtain the required large length of a timber element as well as to perform required interventions and repairing works in the existing timber structures. Notably, most researchers who investigated timber joints reached the conclusion that further experimental and numerical research is needed to learn more about the most appropriate strengthening and repairing techniques for the joints. At the same time, not much research has been done on how to strengthen timber joints with CFRP materials, even though using these materials to strengthen wood elements has shown promising

results. Therefore, this article investigates experimentally different techniques to strengthen the lap joints subjected to bending in glulam timber beams using CFRP sheets to find out the more effective technique that can strengthen such lap joints and achieve the better load transfer and integrity between the joined elements. Continuous nonspliced timber beam and spliced timber beams with strengthened and not strengthened half height lap joints were experimentally tested to examine the ultimate load, failure modes, and effective flexural stiffness. The factors, such as the clamping scheme, bond length, and reinforcement ratio of CFRP sheets that affect the structural behavior of the lap joint will be studied. As the literature survey demonstrated, there are only limited descriptions of research and analyses of strengthening such joints using FRP products. That is what makes the information in the paper novel, and it also represents the author's contribution to the development of this field of science.

2 Materials and methods

2.1 Test beams

Twelve homogeneous glulam timber beam specimens were included in this study. Each beam had overall dimensions of 70 mm in width, 120 mm in height, and 1,500 mm in length and was made of six laminates manufactured by HS Timber Group. The bending strength of the glulam timber beams was 46.5 MPa, and the compressive strength was 39 MPa. The tests were carried out in accordance with EN 408 [32]. One timber beam specimen was an intact nonspliced beam without any lap joints, while the other 11 timber specimens were spliced beams. Each spliced

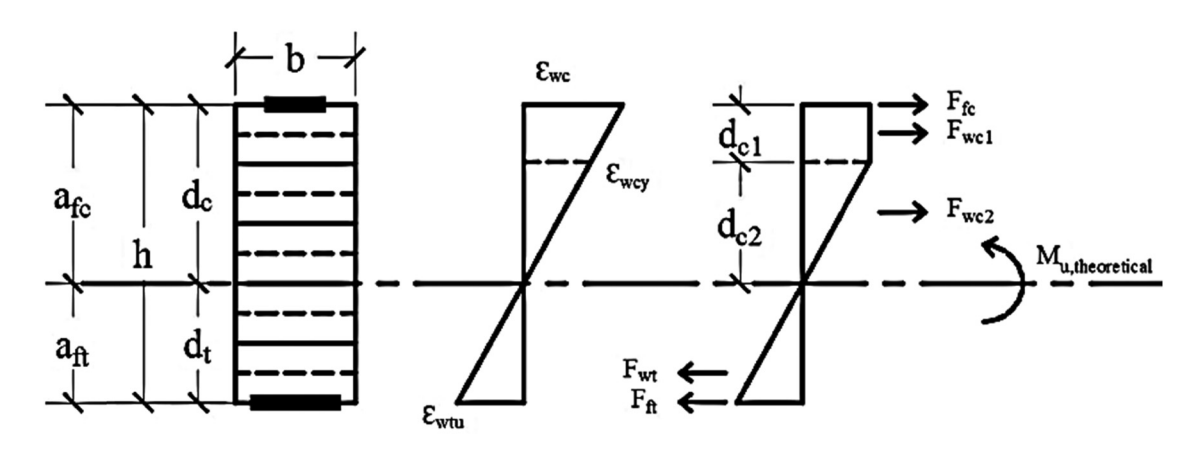


Figure 2: Equilibrium of the strengthened timber beam cross section [31].

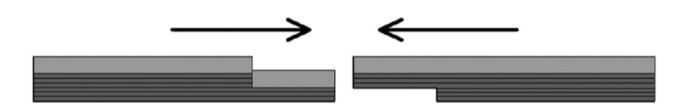


Figure 3: Half-height lap joint.

timber beam was constructed of two elements joined together by means of a half-height lap joint at mid-span, where the interface plane was parallel to the axis of the joined pieces as the wood of one-half of the cross-section height of each piece was removed, as shown in Figure 3. The joint was set at mid-span in the region of maximum bending moment to make sure that the joint is subjected to bending and the behavior of the joint under bending governs the behavior of the whole beam. The lapped parts of each spliced beam were glued using PVA water-based glue at the interface plane without the use of any bolts to avoid stress concentration near the bolt hole. The lapped parts were held together and pressured using manually activated clamps until the glue had completely cured. One spliced timber beam was tested without any additional strengthening. The remaining ten spliced timber beams were strengthened using different clamping schemes of CFRP sheets bonded around the beam cross section and different bond lengths and reinforcement ratios of longitudinal CFRP sheets stuck on the beam bottom face. The details of the tested timber specimens are described in Table 1 and Figure 4. Figure 4a illustrates the drawing details of the specimen B2 (S) that was spliced at midspan without any strengthening. The joint length was equal

to 240 mm, which was designed to be 2 times the specimen depth. The joint length of 240 mm was kept constant in all the spliced specimens. Figure 4b shows the design drawing of specimen B3 (SW28), which was strengthened by fully wrapping the joint using a 280-mm-wide CFRP strip. The design drawing of specimen B4 (SIW9) is shown in Figure 4c. The joint of this specimen was strengthened using two inclined wrapping CFRP strips. The width of each strip was 90 mm. Each strip was inclined by 45° relative to the longitudinal axis of the specimen. The strips were stuck orthogonally to each other so that each strip covered the lower vertical interface plane of the joint on each side of the specimen. At the same time, both inclined strips were passed over the lower horizontal interface plane on the bottom of the specimen. Figure 4d illustrates the design details of the specimens B5 (SL48P1) and B6 (SL72P1). The specimen B5 (SL48P1) was strengthened using a longitudinal CFRP strip of 480 mm long bonded on the bottom side so that the strip extended 120 mm (equal to the specimen depth) outside the joint on each side. One U-shaped CFRP sheet of 50 mm wide was stuck at each end of the longitudinal strip as an anchoring technique. The only difference between specimens B5 (SL48P1) and B6 (SL72P1) was the bonded length of the longitudinal CFRP strip. In the B6 (SL72P1), the bonded length was equal to 720 mm, which means the longitudinal strip extended 240 mm (equal to twice the specimen depth) outside the joint on each side. Figure 4e shows the design details of the specimens B7 (SW28L48P1) and B8 (SW28L72P1). The specimen B7 (SW28L48P1) was strengthened using both the longitudinal strengthening

Table 1: Details of the tested timber beam specimens

Specimens symbol*	Joint length (mm)				CFRP	sheet		
		Wrap		Longitudinal on bottom face				
		Angle (°)	Width (mm)	Length (mm)	Width (mm)	Plies	Area of CFRP (%)	Width of U-sheet at each end (mm)
B1 (NON.S)	_	_	_	_	_	_	_	_
B2 (S)	240	_	_	_	_	_	_	_
B3 (SW28)	240	90	280	_	_	_	_	_
B4 (SIW9)	240	45	90	_	_	_	_	_
B5 (SL48P1)	240	_		480	70	1	0.152	50
B6 (SL72P1)	240	_		720	70	1	0.152	50
B7 (SW28L48P1)	240	90	280	480	70	1	0.152	50
B8 (SW28L72P1)	240	90	280	720	70	1	0.152	50
B9 (SW28L48P2)	240	90	280	480	70 + 70	2	0.303	50
B10 (SW28L72P2)	240	90	280	720	70 + 70	2	0.303	50
B11 (SW48L72P1)	240	90	480	720	70	1	0.152	50
B12 (SW48L72P2)	240	90	480	720	70 + 70	2	0.303	50

^{*}S: Spliced beam, W: Wrapping sheet, IW: Inclined wrapping sheet, L: Longitudinal sheet, P1: 1 Ply of longitudinal sheet, P2: 2 Plies of longitudinal sheet, number after the letter "W": Width of Wrapping sheet in cm, and number after the letter "L": Length of Longitudinal sheet in cm.

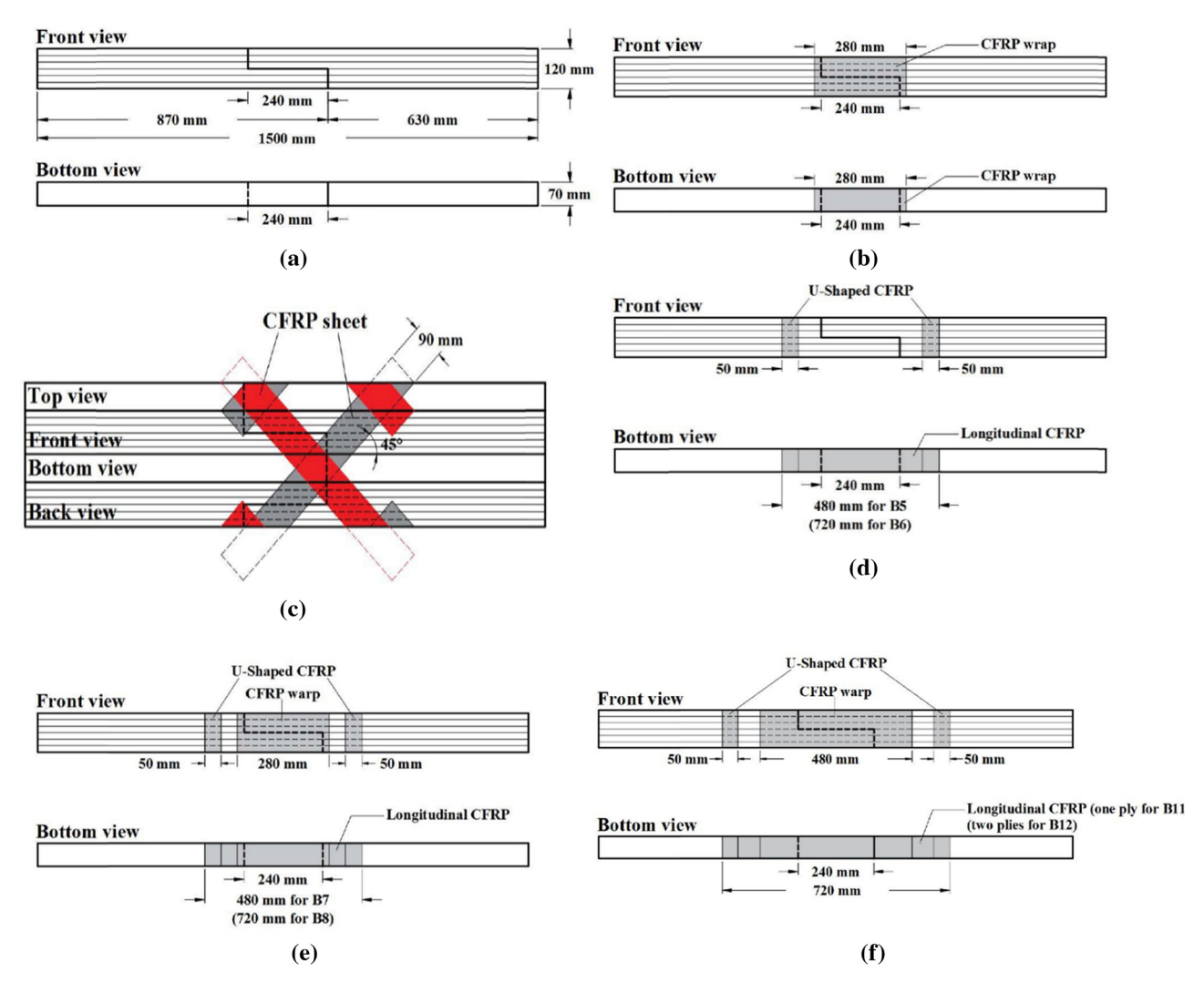


Figure 4: Design drawings of the tested timber specimens. (a) Specimen B2 (S). (b) Specimen B3 (SW28). (c) Specimen B4 (SIW9). Gray strip was installed first and then red strip was installed. (d) Specimens B5 (SL48P1) and B6 (SL72P1). (e) Specimens B7 (SW28L48P1) and B8 (SW28L72P1). (f) Specimens B11 (SW48L72P1) and B12 (SW48L72P2).

scheme used in B5 and the wrapping scheme used in B3. The only difference between specimens B7 (SW28L48P1) and B8 (SW28L72P1) was the bonded length of the longitudinal strips, as described between specimens B5 and B6. The strengthening schemes of specimens B9 (SW28L48P2) and B10 (SW28L72P2) were similar to those of specimens B7 and B8, respectively, but with an additional ply of the CFRP longitudinal strip in each one. Finally, Figure 4f illustrates the drawing details of the specimens B11 (SW48L72P1) and B12 (SW48L72P2). In the specimen B11 (SW48L72P1), the width of the wrapping CFRP strip was 480 mm, which means the wrapping CFRP strip was extended 120 mm (equal to the specimen depth) beyond the joint on each side. In addition to the longitudinal CFRP strip of 720 mm long bonded on the bottom side, one U-shaped CFRP sheet of 50 mm wide was provided at each end. The only difference between specimens B11 (SW48L72P1) and B12 (SW48L72P2) was using an additional ply of the longitudinal CFRP strip in specimen B12.

2.2 CFRP sheets and epoxy resin

The used CFRP sheets were 300 C carbon fiber fabric produced by Sika Group (Switzerland), and the bonding agent that was used to stick the CFRP sheet on wood was Sikadur 330 epoxy resin produced by Sika Group (Switzerland). The properties of the used CFRP sheets and epoxy resin are presented in Tables 2 and 3, respectively.

The CFRP sheets were installed on the wood using a "dry lay-up process" technique. The surface of the timber specimen was treated with sandpaper and thoroughly cleansed of any potential re-deposited particles before

6 — Haider Ali Al-Tameemi et al. DE GRUYTER

Table 2: Properties of CFRP sheet

Туре	Area density (g/m²)	Thickness (mm)	E _{in-tension} (GPa)	Tensile strength (MPa)	Elongation at break
Unidirectional Sika-Wrap®-300 C	304	0.167	230	4,000	1.7%

Table 3: Properties of epoxy resin

Туре	Density (kg/lt)	E _{tension} (MPa)	Tensile strength (MPa)	Elongation at break
Sika-dur [®] -330	1.31	4,500	30	0.9%

applying the epoxy. The two parts of the epoxy resin were mixed according to the manufacturer's datasheet. The epoxy resin was applied concurrently to both the CFRP sheet and the timber surface. After that, a CFRP sheet was put on the timber surface. The CFRP sheet was then lightly pressed using a metallic roller. In the case of the specimens strengthened with more than one ply of CFRP sheets, the new ply was applied to the latter ply after being epoxy-impregnated in the so-called the wet-on-wet procedure.

3 Instrumentation and test procedure

The testing of the timber beam specimens was performed in the structural laboratory of the Faculty of Engineering at the University of Kufa. All the tested timber beams were examined under a four-point loading setup to make the middle third of the specimen span under pure bending. A hydraulic machine of 2,000 kN capacity was used to

conduct the tests, with a loading rate of 2.5 kN/min. The vertical displacement at the middle of the timber beam was measured using a digital dial gauge of 50 mm capacity. The testing arrangement is shown in Figure 5.

4 Results

With the goal of gaining a better understanding and realizing appropriate interpretations for the outputs of the tests carried out in this study, the experimental data are presented and discussed in terms of loading, midspan vertical displacement response, failure mode, and effective stiffness. Particularly, this work focused on studying the effects of various CFRP sheet-strengthening techniques on the flexural behavior of the spliced glulam timber beam specimens. Consequently, additional tables and graph illustrations are provided and analyzed to offer reliable estimates of the improvement in the flexural behavior of the spliced glulam timber beams that was achieved due to these strengthening schemes.

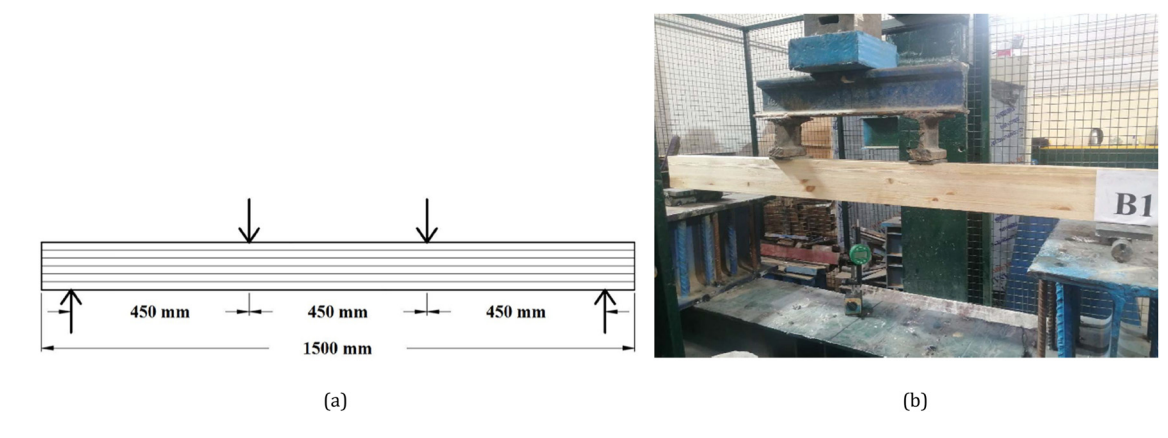


Figure 5: Testing arrangement. (a) Schematic view of 4-point-loading setup. (b) View of a specimen on the test stand.

4.1 Load and vertical mid-span displacement responses

To properly study the structural behavior of the spliced timber beam specimens, the relationship between the loading values of each tested timber beam and their corresponding vertical mid-span displacements was plotted in a graphical representation as shown in Figure 6. Hence, 12 curves are shown in Figure 6, one for each timber specimen. The ordinate of this figure corresponds to the values of the applied load on the timber beams, and its abscissa corresponds to the corresponding vertical midspan displacement values. To enable direct comparison of the outcomes of all the tests, the 12 curves are plotted on a single graph. Moreover, Table 4 lists the outcomes of ultimate loads and associated values of ultimate vertical displacement for the tested glulam timber beams. The ultimate load and vertical displacement at mid-span for the control nonspliced beam B1 (NON.S) were 33 kN and 17.5 mm, respectively, while the spliced nonstrengthened beam B2 (S) failed prematurely at a load of 3.6 kN and a mid-span deflection of 6.28 mm. The ultimate load values for the spliced timber beams with wrapped joints B3 (SW28) and B4 (SIW9) were 15.6 and 18.6 kN, respectively. The load-vertical displacement curves of these two beams, B3 and B4, were running near each other in a similar manner and produced larger vertical displacements among other tested specimens, which were 21.4 mm for B3 and 22.19 mm for B4. The curves for spliced specimens with

bottom-strengthened joints B5 (SL48P1) and B6 (SL48P1) were running together and stiffer than those of B3 and B4 until the load of 10 kN, and then the curve of specimen B6 deviated from that of specimen B5 and failed at a load of 13.6 kN. The specimen B5 continued to gain load until it failed at a load of 16 kN. The load-vertical displacement responses for the spliced specimens with both bottom-strengthened and wrapped joints B7 (SW28L48P1) and B8 (SW28L72P1) were stiffer than those of specimens with either only wrapping or only bottom strengthening. The response of specimen B8 was nearly similar to that of specimen B7 up to a load of 18 kN, when the B8 suffered from an excessive increase in the deflection and failed while the specimen B7 continued gaining load until it failed at a load of 25 kN. The responses for the spliced specimens with wrapped and double bottom-strengthened joints B9 (SW28L48P2) and B10 (SW28L72P2) were running together and stiffer than that of the control nonspliced specimen B1 until the load of 22.5 kN. Then the curve of specimen B10 deviated from that of specimen B9 until a load of 28 kN was reached when this specimen failed after an excessive increase in the deflection. While specimen B9 continued to gain a consentient increase in the load and deflection, it failed at a load of 28 kN, which is less than that of the control nonspliced specimen B1 (33 kN). For the specimen B11 (SW48L72P1), which was similar to the B8 but with a wider wrap (48 mm), the load-vertical displacement response was nearly coinciding with that of the control nonspliced specimen B1 till the load of 22 kN, and then it descended

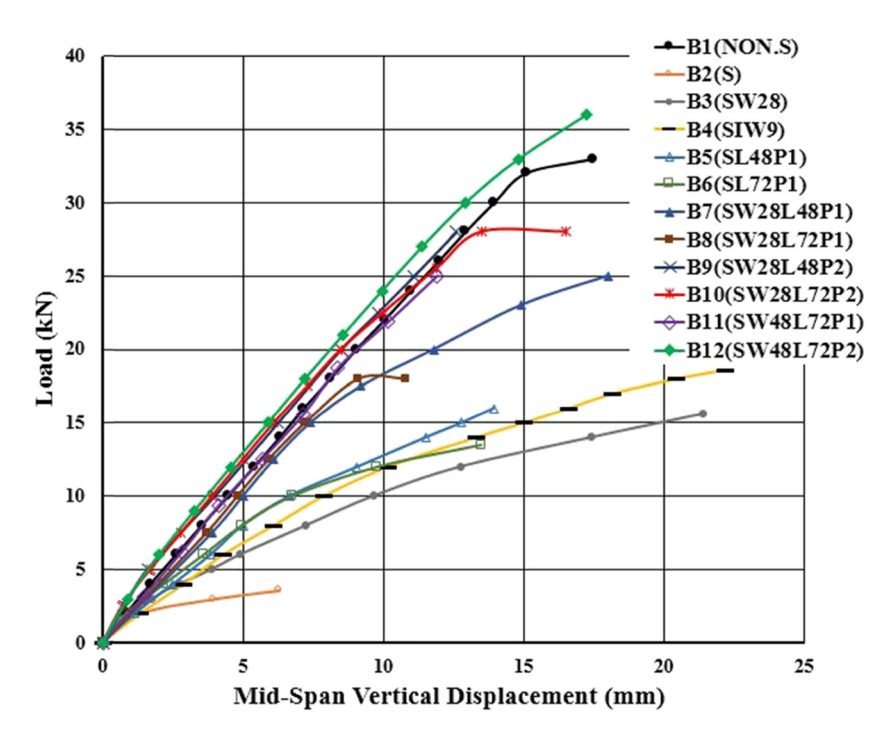


Figure 6: Load versus mid-span vertical displacement for the tested glulam timber specimens.

 Fable 4: Test results for tested glulam timber specimens

Specimen	Ultimate load, Pu (kN)	Ultimate deflection (mm)	(Pu);/(Pu) _{B1} *	Failure mode
B1 (NON.S)	33	17.5	1.00	Simple tension in lower side of the beam (Flexural failure)
B2 (S)	3.6	6.28	0.11	Joint loosening
B3 (SW28)	15.6	21.4	0.47	Delamination crack between upper and lower parts of the beam at side of the joint
B4 (SIW9)	18.6	22.19	0.56	Bond failure followed by rupture of inclined wrapping CFRP sheet
B5 (SL48P1)	16	13.92	0.48	Bond failure of longitudinal CFRP sheet
B6 (SL72P1)	13.5	20	0.41	Bond failure of longitudinal CFRP sheet
B7 (SW28L48P1)	25	18	0.76	Bond failure of longitudinal CFRP sheet followed by delamination crack at side of the joint
B8 (SW28L72P1)	18	10.8	0.55	Delamination crack between upper and lower parts of the beam at side of the joint
B9 (SW28L48P2)	28	11.5	0.85	Bond failure of longitudinal CFRP sheet
B10 (SW28L72P2)	28	16.5	0.85	Bond failure of longitudinal CFRP sheet followed by delamination crack
B11 (SW48L72P1)	25	11.91	0.76	Rupture of longitudinal CFRP sheet
B12 (SW48L72P2)	36	17.23	1.10	Bond failure of longitudinal CFRP

*(Pu); failure load of considered timber beam, (Pu)_{B1}; failure load of control timber beam

more and the specimen failed at a load of 25 kN. For specimen B12 (SW48L72P2), which was similar to B10 but with a wider wrap (48 mm), the response was stiffer than all those of the other tested timber beams, even than that of the control non-spliced specimen B1; it failed at an ultimate load and vertical displacement of 36 kN and 17.23 mm, respectively.

4.2 Mode of failure

Table 4 lists also the failure mode of each tested glulam timber beam. Figure 7 presents the failure modes of the tested specimens. According to Figure 7a, the tension failure of the wood fibers on the underside of the control beam B1 caused it to fail. This type of failure is referred to as simple tension and is a flexural failure [33,34]. The nonstrengthened spliced timber specimen B2 separated early into two segments due to joint loosening without any evidence of tensile or compressive failure but rather due to failure of glue material at the horizontal plane of the lap joint, as shown in Figure 7b. The spliced specimen with fully wrapped joint B3 failed due to a delamination crack that initiated at the right part of the lap joint. This crack led to the separation of the lower part (timber laminates) of the right segment and the opening of the lower seam of the joint. The failure of specimen B4 was characterized by debonding in the inclined CFRP sheet along the lower vertical interface of the joint, followed by rupture of this inclined sheet at the lower corners of the lap joint, which coincided with opening the lower seam of the joint. The bond failure was also prevalent in both B5 and B6 specimens. In each of these specimens, the left part of the joint moved downward relative to the right part of the joint. The bond failure of B5 was marked by the delamination of some of the lower wooden fibers with the CFRP sheet. In specimen B6, the bond failure occurred at the interface between the CFRP sheet and wood surface to the right of the joint seam. The delamination crack between the lower and upper parts of the right segment was the main reason for the failure mode of specimens B7 and B8. The failure of B7 was preceded by signs of debonding in the longitudinal CFRP sheet, while no evidence of debonding was marked in specimen B8. Although the bonded length of specimen B8 was larger than that of specimen B7, the failure load of B8 was smaller than that of B7. For specimens B9, the failure was due to debonding of longitudinal CFRP plies, which led to tearing the wrapping and clamping CFRP sheets at the right of the joint. While for specimen B10, the failure was due to debonding of longitudinal CFRP plies and a delamination crack between the lower and upper parts of the right segment. Furthermore, for specimen B11, the failure occurred

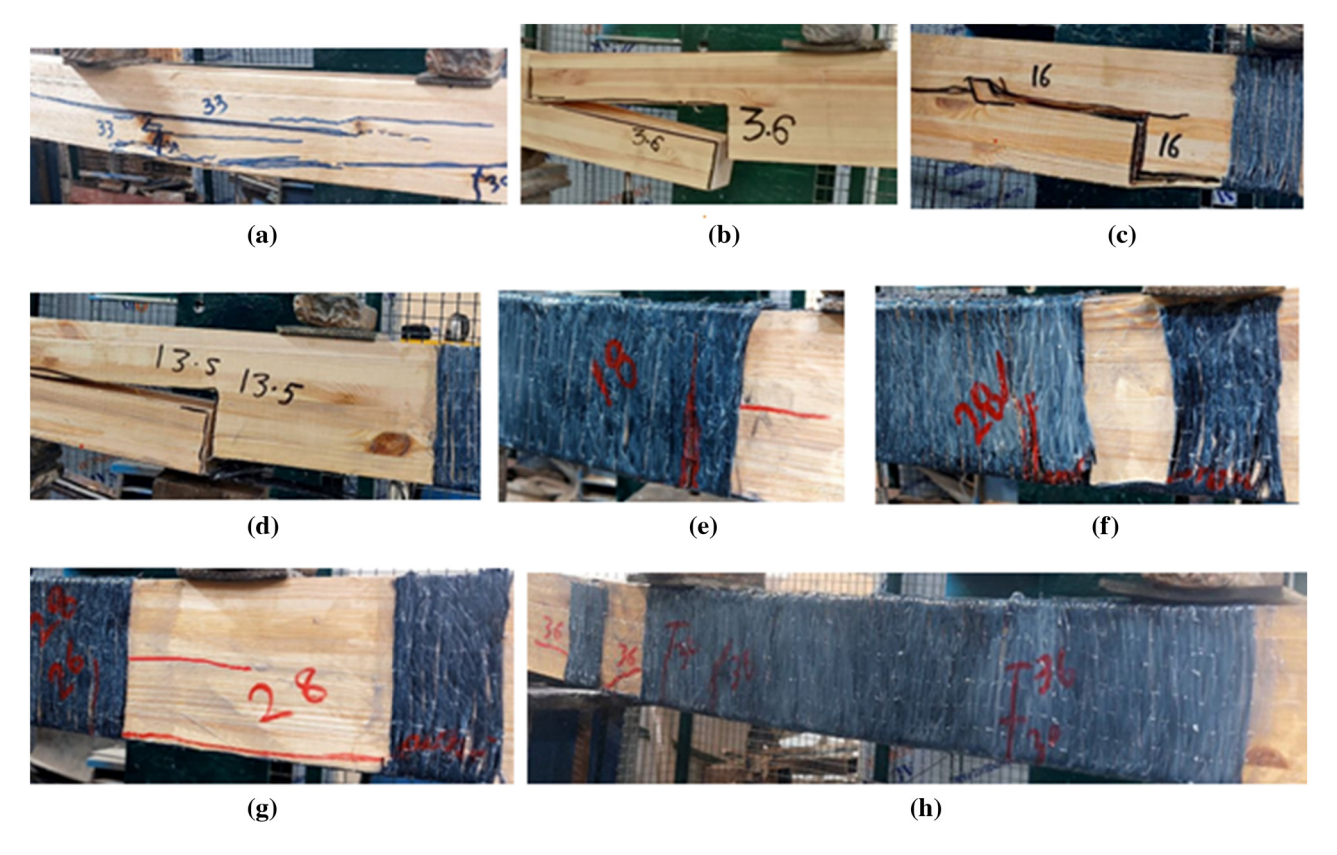


Figure 7: Failure mode of tested glulam timber specimens. (a) B1. (b) B2. (c) B5. (d) B6. (e) B8. (f) B9. (q) B10. (h) B12.

owing to rapture of the single longitudinal underside CFRP ply at the lower seam of the joint without any marked signs of debonding or delamination crack. Finally, for specimen B12, the failure was governed by debonding cracks outside the jointed region at the end of the longitudinal underside CFRP sheets, which coincided with flexural cracks within the maximum constant bending moment region.

4.3 Effective stiffness

For the structural members, the effective stiffness can be estimated based on the load-displacement plots as the slope of the line crossing the point where the applied force reaches 75% of the nominal strength. Thus, the effective stiffness can be expressed as in equation (2) [35].

Table 5: Details of the effective stiffness for tested glulam timber beams

Specimen	Pu (kN)	0.75Pu (kN)	$\Delta_{0.75Pu}$ (mm)	$K_{\rm eff}$ (kN/mm)	$(K_{\rm eff})_{\rm i}/(K_{\rm eff})_{\rm B1}^{\star}$
B1 (NON.S)	33	24.75	11.38	2.175	1
B2 (S)	3.6	2.70	3.13	0.863	0.40
B3 (SW28)	15.6	11.70	12.38	0.945	0.43
B4 (SIW9)	18.6	13.95	13.25	1.053	0.48
B5 (SL48P1)	16	12.00	9.12	1.316	0.60
B6 (SL72P1)	13.5	10.13	6.63	1.527	0.70
B7 (SW28L48P1)	25	18.75	10.60	1.769	0.81
B8 (SW28L72P1)	18	13.50	6.50	2.077	0.95
B9 (SW28L48P2)	28	21.00	9.13	2.300	1.06
B10 (SW28L72P2)	28	21.00	9.13	2.300	1.06
B11 (SW48L72P1)	25	18.75	8.38	2.237	1.03
B12 (SW48L72P2)	36	27.00	11.38	2.373	1.09

^{*} $(K_{\rm eff})_{\rm i}$: effective stiffness of considered timber beam, $(K_{\rm eff})_{\rm B1}$: effective stiffness of control timber beam B1.

$$K_{\rm eff} = 0.75 \,\mathrm{Pu}/\Delta_{0.75 \,\mathrm{Pu}},$$
 (2)

where $K_{\rm eff}$ is the effective stiffness of the tested timber glulam beam in kN/mm, Pu is the ultimate load of the tested timber glulam beam in kN, and $\Delta_{0.75{\rm Pu}}$ is the midspan vertical displacement of the tested timber glulam beam corresponding to 0.75Pu.

The details of the effective stiffness for the tested timber beams are listed in Table 5. Figure 8 illustrates a comparison between the effective stiffness values of each tested specimen. Based on Table 5 and Figure 8, it is clear that the effective stiffness of the glulam timber beam dropped drastically due to the presence of a nonstrengthened lap joint, as in the specimen B2 (S). It is noticed that the strengthening schemes containing only CFRP wrapping sheets could not succeed in achieving a considerable enhancement in the effective stiffness of the spliced glulam timber beams, as in specimens B3 (SW28) and B4 (SIW9). Although it was noted that the improvement in the effective stiffness values for specimens with only underside strengthening CFRP sheets, as in B5 (SL48P1) and B6 (SL72P1) beams, was better than that due to only wrapping CFRP sheets, it is still not large enough to recover the effective stiffness of the spliced specimens. It is clearly observed that the increases in the stiffness value were more pronounced when the strengthening schemes of the spliced beams consisted of the longitudinal underside and wrapping CFRP sheets. The effective stiffness values of spliced specimens B7 (SW28L48P1) and B8 (SW28L72P1) were 81 and 95%, respectively, of that of the nonspliced one. Moreover, the effective stiffness values were higher than that of the nonspliced one for the spliced specimens B9 (SW28L48P2), B10 (SW28L72P2), B11 (SW48L72P1), and B12 (SW48L72P2). The largest improvement

in the effective stiffness was achieved for B12 (SW48L72P2), where it was 1.09% of that of the nonspliced intact specimen.

5 Discussion

The failure of the control intact beam B1 was a typical tension-controlled flexural failure. This failure can be attributed to that the flexural tensile stresses exceeded the tensile strength of wooden fibers on the lower side of the timber beam in the region of the maximum bending moment. On the other hand, the joint loosening that occurred in the nonstrengthened spliced specimen B2 was due to the failure of the bonding material along the joint's horizontal plane between the opposite surfaces of the lapped segments. As there was no other component that could counteract the flexural tensile stresses that developed in the lower part of the joint. Therefore, this specimen exhibited weak stiffness and failed prematurely.

5.1 Effect of CFRP wrapping sheets

To study the influence of wrapping the joint with CFRP sheets on the behavior of the spliced glulam timber beams, the load-vertical displacement curve of nonstrengthened spliced beam B2 is plotted in Figure 9 versus those curves of B3 and B4, which were strengthened with vertical and 45° inclined CFRP wrapping sheets, respectively. Although it is seen that the wrapping of the joint could improve the

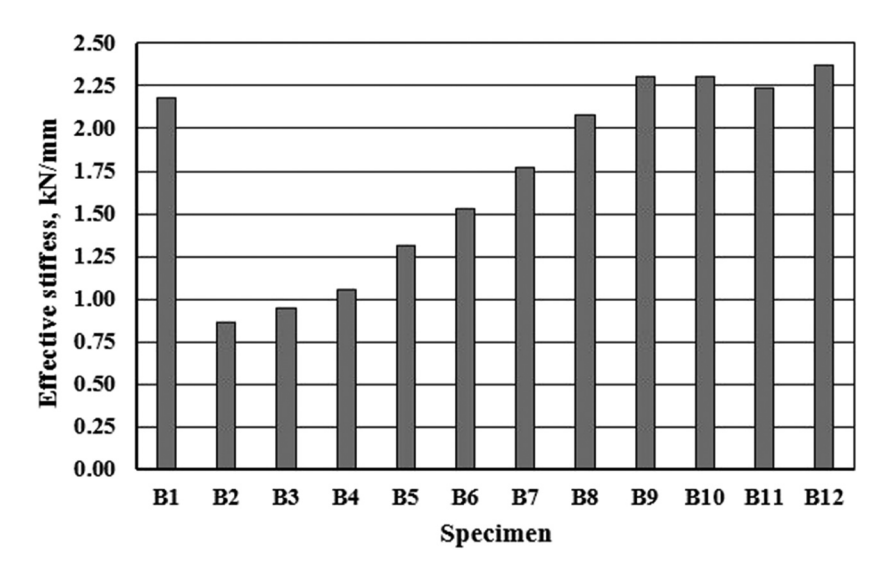


Figure 8: Effective stiffness for tested beams.

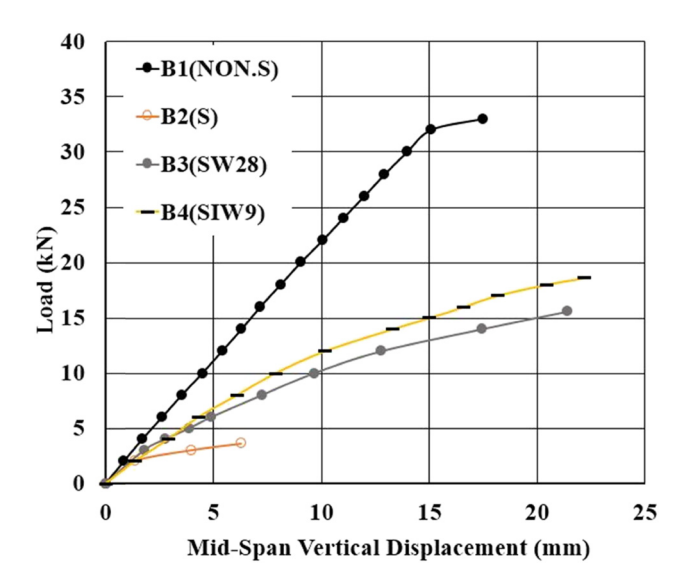


Figure 9: Effect of CFRP wrapping sheets.

DE GRUYTER

structural behavior of the lapped beams, the failure loads increased by 36 and 45% for B3 and B4, respectively, compared with the control intact beam. The corresponding increases in effective stiffness were 3 and 8%. However, it is clear that the strengthening schemes involving only wrapping the joint were not adequate to achieve the required improvement in the structural behavior of the spliced timber beams. This can be interpreted by saying that when the CFRP sheet wrapped the joint, it clamped the spliced parts together and prevented any relative movement between them. On the other hand, as the applied load increased, the lower seam of the joint started to open because of flexural tensile stresses at the underside of the beam. As a result, at the right of the joint, only the upper half of the cross section was able to withstand the flexural stresses, which caused delamination between the upper and lower parts of the right segment and reduced its effective depth, as illustrated in Figure 10.

The load transfer and stress concentrations through the abrupt change in the depth of the timber beam at the joint can be interpreted by means of the "structural element model" that was proposed by Serrano et al. [36,37]. This model is assumed to be consisted of two Timoshenko

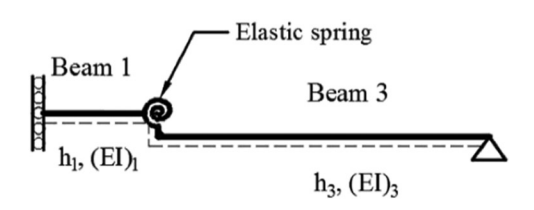


Figure 11: Structural element model suggested by Serrano et al. [36,37].

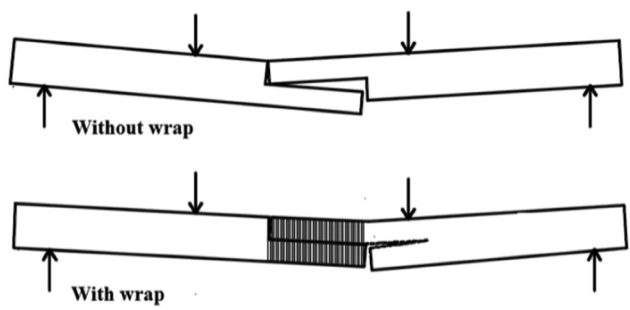


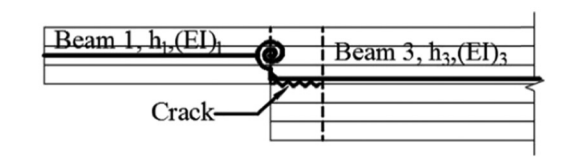
Figure 10: Joint loosening and delamination failure modes.

beam elements jointed by an elastic spring and a fictitious rigid rod as shown in Figure 11. The lapped part of the right segment can be represented by beam 1, and the entire nondelaminated (un-cracked) cross section of the right segment in front of the crack is represented by beam 3. The additional rotation at the tip of the delamination crack is simulated by the elastic spring, which results in increased distortion and compliance.

Why the specimen with 45° inclined CFRP sheets gave better strengthening than that of the vertical CFRP sheet may be attributed to the fact that, in addition to the clamping vertical component, the inclined sheets provided a horizontal component that contributed to resisting tensile stresses. Moreover, the inclined sheets were extended at the right of the joint, which counteracted the delamination between the upper and lower parts of the right segment. It is important to mention that the installation of the inclined sheets was more difficult than that of the vertical sheets, and the total surface area of the CFRP sheets used in the inclined wrap was larger than that used in the vertical wrap by about 18%.

5.2 Effect of CFRP longitudinal underside sheets

The load-vertical displacement curves of spliced timber beams with different bonded lengths of longitudinal underside CFRP sheets, namely, 480 and 720 mm, were plotted in



12 — Haider Ali Al-Tameemi et al. DE GRUYTER

Figure 12 together with those of the intact and nonstrengthened spliced beams to study the influence of strengthening the joint with the underside CFRP sheets on the behavior of the spliced glulam timber beams. It is noted that the failure load of the spliced timber beam increased by 37 and 30% due to strengthening the lapped region with longitudinal underside CFRP sheets of lengths of 480 mm (for beam B5) and 720 mm (for beam B6), respectively, compared with the control intact beam. The corresponding increases in effective stiffness were 20 and 30%. In general, the improvement in the structural behavior of the lapped timber beams due to this strengthening scheme can be ascribed to that the underside CFRP sheet tied the opposite sides of the joint lower seam and contributed to counteracting the flexural tensile stresses. However, the underside CFRP sheets debonded at relatively low load values. This is due to that the left lapped part deflected downward and thereby caused the peeling off of the CFRP sheet from the right part, as shown in Figure 7d. Moreover, it is observed that specimen B5 that was strengthened with the shorter CFRP sheet (480 mm) endured an ultimate load value higher than that of specimen B6 that was strengthened with the longer CFRP sheet (720 mm). This can be interpreted by that in the case of the CFRP sheet length of 480 mm, the U-shaped CFRP sheets, which were installed at the ends of the longitudinal CFRP sheet, were closer to the joint than those in the case of a sheet length of 720 mm and thereby provided better anchorage against the peeling off stresses.

5.3 Effect of combination of wrapping and underside CFRP sheets

To study the effect of strengthening the lap joint with both wrapping and longitudinal underside CFRP sheets on the behavior of spliced timber beams, the load-vertical displacement curves of spliced beams with such strengthening schemes are plotted together with those curves of spliced beams with wrapping CFRP sheet only or with longitudinal underside CFRP sheet only in Figure 13. It is clear that strengthening the joint with both wrapping and longitudinal underside CFRP sheets made the improvement in the structural behavior of the spliced timber beams more pronounced and significant than when the joint was strengthened with either wrapping or longitudinal underside CFRP sheets. The ultimate load and the effective stiffness of the spliced beams increased due to using such strengthening schemes up to 65 and 55%, respectively, compared with the control intact beam. This is because this strengthening scheme, in addition to clamping the lapped horizontal parts,

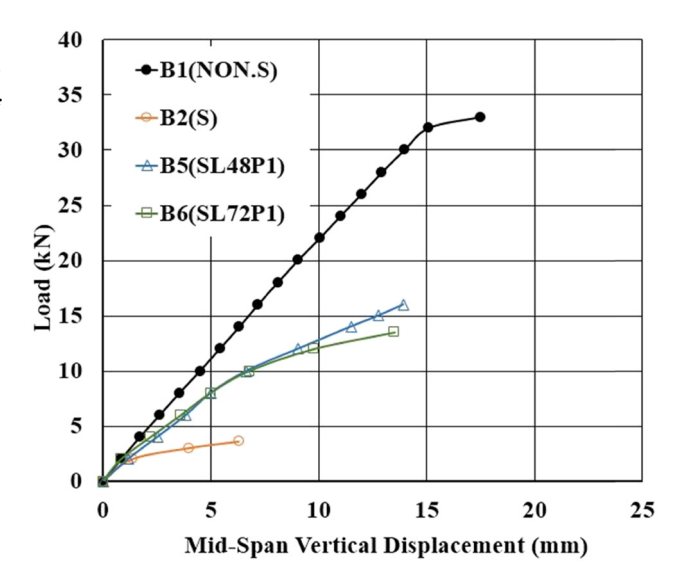


Figure 12: Effect of CFRP longitudinal underside sheets.

tied the vertical sides of the lower seam of the joint and contributed to resisting the tensile stresses and improving the integrity of the joined segments. It was noticed again that the specimen of shorter underside CFRP sheet B7 gave a higher ultimate load (25 kN) than that of the specimen of longer underside CFRP sheet B8 (18 kN). This can be attributed to that in the specimen with the longer underside sheet, the U-shaped anchorage CFRP sheets were relatively far away from the joint and did not contribute to preventing or delaying the delamination between the upper and lower halves of the right segment, which weakened the specimen at the right segment by reducing its effective depth. On the other hand, in the specimen with the shorter underside

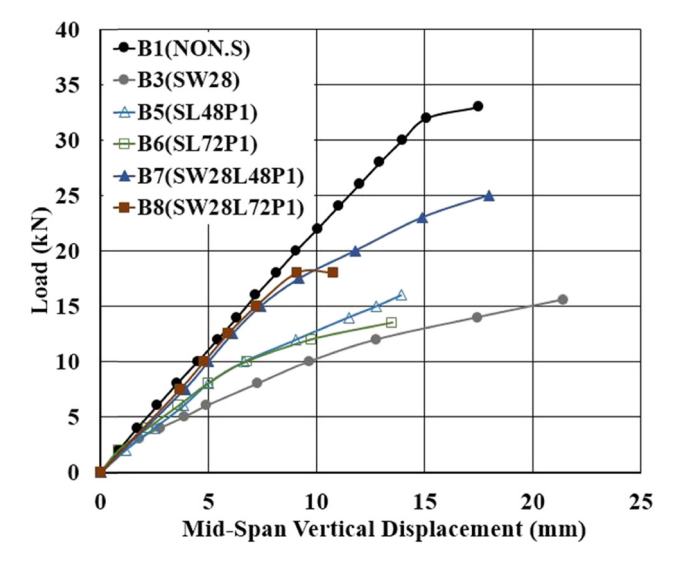


Figure 13: Effect of wrapping and underside CFRP sheets.

sheet, the U-shaped anchorage CFRP sheets were relatively near the joint and delayed the delamination between the upper and lower halves of the right segment. When this specimen reached a relatively higher load value (21 kN), the short underside CFRP sheet underwent signs of debonding failure, which weakened the joint and then caused the delamination failure at the load value of 25 kN.

5.4 Effect of increasing reinforcement ratio of the underside CFRP sheets

To inspect the influence of increasing the reinforcement ratio of the longitudinal underside CFRP sheets on the structural behavior of the spliced timber beams, the loadvertical displacement curves of spliced timber beams with one and two plies of the underside CFRP sheets were plotted together in Figure 14 in comparison with that of the intact beam. Figure 14 shows clearly that increasing the area ratio of the underside CFRP sheets led to increasing the flexural stiffness of spliced timber beams. The effective stiffness of specimens B9 and B10 with a CFRP area ratio of 0.303% (with different bonded lengths) increased by 30 and 11%, respectively, relative to the corresponding specimens with a CFRP area ratio of 0.152%. The corresponding increases in the ultimate failure load were 12 and 56%, respectively. Generally, these enhancements can be attributed to that increasing the CFRP area ratio by using an additional CFRP ply resulted in an increase in the area of the component that resists tensile stresses and ties between the opposite sides of the joint lower seam. Thereby, this led

to improving the joint integrity and reducing the deflection and the relative movement between the lapped parts. It is also noticed that specimen B10 exerted a relatively excessive vertical displacement before the failure. This can be ascribed to the fact that the failure of specimen B10 occurred in two steps: debonding followed by delamination. The effect of the U-shaped anchorage CFRP sheet near the joint in the specimen of the shorter underside CFRP sheets (B8) was also marked where it could prevent the delamination in the right segment.

5.5 Effect of increasing the width of CFRP wrapping sheet

Figure 15 was plotted to study the influence of increasing the width of the CFRP wrapping sheet on the structural behavior of the spliced timber beams. Figure 15 includes the load-vertical displacement curves of the specimens with CFRP wrapping sheets of 48 mm width (B11 and B12) together with those curves of the corresponding specimens with CFRP wrapping sheets of 28 mm width (B8 and B10). It is clear that increasing the width of the CFRP wrapping sheets led to increases in the flexural effective stiffness and ultimate load values of the spliced timber beams. The ultimate load and effective stiffness of specimen B11 (with a single ply of longitudinal underside CFRP sheet) increased by 39 and 8%, respectively, relative to those of the corresponding specimen B8. As well, the failure mode was changed from the delamination crack in specimen B8 to the rapture of the longitudinal underside CFRP sheet in

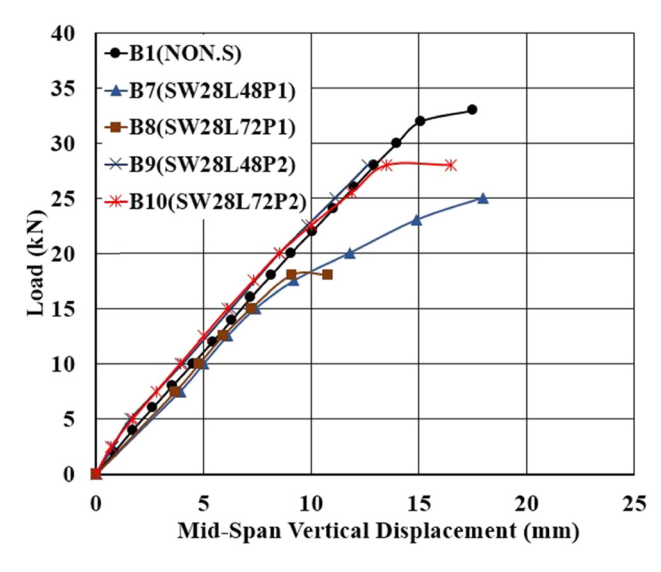


Figure 14: Effect of reinforcement ratio of the underside CFRP sheets.

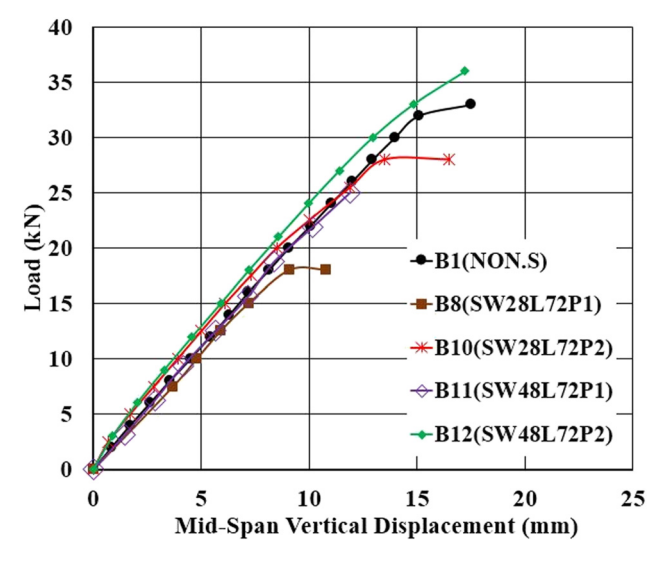


Figure 15: Effect of the width of CFRP.

specimen B11. The effect of increasing the width of CFRP wrapping sheets was more significant in specimen B12 (with double plies of longitudinal underside CFRP sheet). The largest improvements in the effective stiffness and ultimate load were achieved in this specimen (B12), where its effective stiffness and ultimate load were higher than those of the nonspliced intact specimen by 9 and 10%, respectively. Moreover, the lapped parts of specimen B12 acted integrally as one unit, and failure occurred outside the region of the constant maximum bending moment. This was because increasing the width of the CFRP wrapping sheets could succeed in providing adequate clamping to the lapped and laminated timber layers in addition to anchoring the longitudinal CFRP sheets along the region of constant maximum bending moment. Consequently, this led to preventing the debonding and delamination failures in the region of constant maximum bending moment and allowed greater use of the tensile strength available in the longitudinal CFRP sheets.

Ultimately, the results of this study conform to the results that were obtained by Ye et al. [10] when they strengthened the lap joints in standard (not laminated) timber beams of circular cross section using CFRP sheets under bending. They could achieve an increase in the ultimate load of the lapped timber beam by 112% relative to that of the intact beam when they increased the CFRP reinforcement ratio to 0.34% and used four clamping CFRP sheets – two at the ends of the lap joint and two at the ends of the longitudinal CFRP sheet in addition to two steel bolts within the joint.

6 Conclusions

The article focused on studying the flexural behavior of glulam timber beams with half height lap joints strengthened using CFRP sheets in terms of ultimate load, failure mode, and effective flexural stiffness. Based on analyzing the experimental results of the 12 adopted specimens, the following can be concluded:

The experimental tests of this study demonstrate the effectiveness of using CFRP sheets in reinforcing the half-height lap joints in glulam timber beams under bending. The findings show that strengthening the half-height lap joints using CFRP sheets led to considerable improvements in the structural behavior of the glulam timber beams that contained such joints.

The experimental data indicate that strengthening the joints with both wrapping and longitudinal underside CFRP sheets made the improvement in the structural

behavior of the spliced timber beams more pronounced and significant than when the joints were strengthened with either wrapping or longitudinal underside CFRP sheets. The longitudinal CFRP sheets tied the vertical opposite sides of the lower seam of the joint and contributed to resisting the tensile stresses, and the wrapping CFRP sheets clamped the lapped horizontal parts and the laminated timber layers, which led to improving the integrality of the joined segments.

Moreover, the results reveal that increasing the length or the reinforcement ratio of the longitudinal CFRP sheets without increasing the width of the wrapping CFRP sheets could not succeed in achieving the required improvements in the structural behavior of the lapped timber beams. More specifically, the results demonstrate that to obtain the greater use of the tensile strength available in the longitudinal CFRP sheets, it was required to increase the width of the wrapping CFRP sheets to be continued outside the joint by a distance equal to the beam height (120 mm). This is because increasing the width of the CFRP wrapping sheets led to adequate clamping of the lapped and laminated timber layers in addition to anchoring the longitudinal CFRP sheets for a sufficient length.

Ultimately, the research found that the configuration of CFRP sheets could be more effective in strengthening the lapped glulam timber beams when the reinforcement ratio of the longitudinal CFRP sheets was equal to 0.303% and the wrapping CFRP sheets continued beyond the joint by a distance equal to the beam height. Such a strengthening configuration could succeed in increasing the effective stiffness and ultimate load of the lapped timber specimen to 109 and 110, respectively, relative to those of the intact nonlapped specimen.

Conflict of interest: The authors state no conflict of interest.

Data availability statement: Most datasets generated and analyzed in this study are comprised in this submitted manuscript. The other datasets are available on reasonable request from the corresponding author with the attached information.

References

- Jasieńko J, Nowak T, Karolak A. Historical carpentry joints. J Herit Conserv. 2014;40:58–82.
- [2] Isharyadi F, Kristiningrum E. Profile of system and product certification as quality infrastructure in Indonesia. Open Eng. 2021 Mar;11(1):556–69. doi: 10.1515/eng-2021-0054.

[3] Schmid J, Frangi A. Structural timber in compartment fires-The timber charring and heat storage model. Open Eng. 2021 Mar;11(1):435-52. doi: 10.1515/eng-2021-0043.

DE GRUYTER

- [4] Patalas F, Karolak A, Nowak TP. Numerical analyses of timber beams with stop-splayed scarf carpentry joints. Eng Struct. 2022 Sep;266:114626. doi: 10.1016/j.engstruct.2022.114626.
- Cepelka M, Malo KA. Review on on-site splice joints in timber engineering. In Proceeding of COST Timber Bridge Conference-CTBC 2014. 2014 Sep. p. 1-8.
- Cepelka M, Malo KA. Moment resisting on-site splice of large glulam elements by use of mechanically coupled long threaded rods. Eng Struct. 2018 May;163:347-57. doi: 10.1016/j.engstruct.
- Karolak A. Jasieńko I. Raszczuk K. Historical scarf and splice carpentry joints: State of the art. Herit Sci. 2020 Dec;8:1-9. doi: 10.1186/s40494-020-00448-2.
- Karolak A. Experimental investigation of timber beams with splice and scarf joints. Constr Build Mater. 2021 Nov;306:124670. doi: 10.1016/j.conbuildmat.2021.124670.
- PN-EN 1995-1-1:2010—Eurocode 5: Design of Timber Structures— Part 1: General- Common Rules and Rules for Buildings. Polish Committee for Standardization: Warsaw, Poland, 2010.
- [10] Ye L, Wang B, Shao P. Experimental and numerical analysis of a reinforced wood lap joint. Materials. 2020 Sep;13(18):4117. doi: 10.3390/ma13184117.
- Karolak A, Jasieńko J, Nowak T, Raszczuk K. Experimental investi-[11] gations of timber beams with stop-splayed scarf carpentry joints. Materials. 2020 Mar;13(6):1435. doi: 10.1016/j.conbuildmat.2021. 124670.
- [12] Fajman P, Máca J. The effect of key stiffness on forces in a scarf joint. In Proceedings of the 9th international conference on engineering computational technology. Vol. 40. 2014 Sep.
- [13] Fajman P, Máca J. Scarf joints with pins or keys and dovetails. In Proceedings of the 3rd International Conference on Structural Health Assessment of Timber Structures—SHATIS. Vol. 15. 2015.
- [14] Fajman P, Máca J. The effect of inclination of scarf joints with four pins. Int J Archit Herit. 2018 May;12(4):599-606.
- [15] Fajman P, Máca J. Stiffness of scarf joints with dowels. Comput Struct. 2018 Sep;207:194-9. doi: COMPSTRUC.2017.03.005">10.1016/I.COMPSTRUC.2017.03.005.
- [16] Arciszewska-Kędzior A, Kunecký J, Hasníková H, Sebera V. Lapped scarf joint with inclined faces and wooden dowels: Experimental and numerical analysis. Eng Struct. 2015 Jul;94:1–8. doi: ENGSTRUCT.2015.03.036">10.1016/J.ENGSTRUCT.2015.03.036.
- [17] Kunecký J, Sebera V, Hasnikova H, Arciszewska-Kędzior A, Tippner J, Kloiber M. Experimental assessment of a full-scale lap scarf timber joint accompanied by a finite element analysis and digital image correlation. Constr Build Mater. 2015 Feb;76:24-33. doi: ENGSTRUCT.2015.03.036">10.1016/J.ENGSTRUCT.2015.03.036.
- [18] Kunecký J, Hasníková H, Kloiber M, Milch J, Sebera V, Tippner J. Structural assessment of a lapped scarf joint applied to historical timber constructions in central Europe. Int | Archit Herit. 2018 May;12(4):666-82. doi: 10.1080/15583058.2018.1442524.
- [19] Karolak A, Jasieńko C. Experimental investigation of scarf joint of 'lightning sign'in bending. In 12th International Conference on Structural Analysis of Historical Constructions - SAHC. 2021. doi: 10.23967/sahc.2021.101.

- [20] Unterweger C, Brüggemann O, Fürst C. Synthetic fibers and thermoplastic short-fiber-reinforced polymers: Properties and characterization. Polym Compos. 2014 Feb;35(2):227-36. doi: 10.1177/ 0731684413516393.
- [21] Sathishkumar TP, Naveen JA, Satheeshkumar S. Hybrid fiber reinforced polymer composites-a review. J Reinf Plast Compos. 2014 Mar;33(5):454-71. doi: 10.1177/0731684413516393.
- [22] Kaiser HP. Strengthening of reinforced concrete with epoxybonded carbon-fiber plastics. Doctoral thesis, Diss. ETH; 1989.
- [23] Ritchie PA, Thomas DA, Lu LW, Connelly GM. External reinforcement of concrete beams using fiber reinforced plastic. Master's thesis. Lehigh University; 1989.
- [24] Saadatmanesh H, Ehsani MR. Application of fiber-composites in civil engineering. Proc Sessions RelStruct Mater Struct Congress' 89. ASCE; 1989. p. 526-35.
- [25] Saad K, Lengyel A. Strengthening timber structural members with CFRP and GFRP: A state-of-the-art review. Polymers. 2022 Jun;14(12):2381. doi: 10.3390/polym14122381.
- [26] Triantafillou TC, Deskovic N. Prestressed FRP sheets as external reinforcement of wood members. J Struct Eng. 1992 May;118(5):1270-84.
- [27] Plevris N, Triantafillou TC. FRP-reinforced wood as structural material. J Mater Civ Eng. 1992 Aug;4(3):300-17.
- [28] De Lorenzis L, Scialpi V, La Tegola A. Analytical and experimental study on bonded-in CFRP bars in glulam timber. Compos Part B: Eng. 2005 Jun;36(4):279-89. doi: 10.1016/j.compositesb.2004.11.005.
- [29] Nadir Y, Nagarajan P, Ameen M. Flexural stiffness and strength enhancement of horizontally glued laminated wood beams with GFRP and CFRP composite sheets. Constr Build Mater. 2016 Jun;112:547-55.
- [30] Al-Katib HA, Alkhudery HH, Al-Tameemi HA. Structural behavior of standard timber beams strengthened using CFRP sheet. Asian J Civ Eng. 2022 Jul;23(5):727-39. doi: 10.1007/s42107-022-00452-w.
- [31] Yeboah D, Gkantou M. Investigation of flexural behaviour of structural timber beams strengthened with NSM basalt and glass FRP bars. Structures. 2021 Oct;33:390-405. Elsevier. doi: 10.1016/j. istruc.2021.04.044.
- [32] EN 408+A1: 2012; Timber structures. Structural timber and glued laminated timber. Determination of some physical and mechanical properties. CEN: Brussels, Belgium; 2012.
- [33] Record S. The mechanical properties of wood. New Haven, USA: Yale University Press; 2004 p. 114.
- [34] Williams K, Chalmers D, Suorineni FT. Assessing the suitability of recycled material as a timber substitute in drawpoint design. J Res Proj Rev. 2015;4(1):73-82.
- [35] Vu NS, Li B, Beyer K. Effective stiffness of reinforced concrete coupling beams. Eng Struct. 2014;76:371-82. doi: 10.1016/j. engstruct.2014.07.014.
- Serrano E, Gustafsson PJ, Danielsson H. Prediction of load-bearing capacity of notched cross laminated timber plates. In International Network on Timber Engineering Research-Meeting 52. Karlsruhe, Germany: Timber Scientific Publishing; 2019.
- Serrano E, Danielsson H. Fracture mechanics based design of CLTplates-notches at supports and half-and-half joints. In International Network on Timber Engineering Research-Meeting 53. Karlsruhe, Germany: Timber Scientific Publishing; 2020. p. INTER-53.